ELSEVIER

Journal of Nuclear Materials 279 (2000) 286–292

journal of nuclear materials

www.elsevier.nl/locate/jnucmat

K_{IH} in radial textured Zr–2.5%Nb pressure tube

Sung Soo Kim *, Young Suk Kim

CANDU Reactor Materials, Korea Atomic Energy Research Institute, P.O. Box 105, Yousung-Ku, Taejon 305-353, South Korea

Received 8 July 1999; accepted 7 December 1999

Abstract

The texture of Zr–2.5%Nb pressure tube was modified by tube expansion using the plain strain fixture to the radial textured one in order to evaluate the effect of texture modification on K_{IH}. The basal pole components were then measured and compared to confirm the texture variation. The K_{IH} in the radial direction appeared to be $\sim$17 MPa$\sqrt{m}$ at 250°C, and this is at least 70% higher than that of conventional pressure tube. This behavior can be explained using the grain orientations and the basal pole component in the cracking plane which is normal to the transverse direction of the pressure tube. The K_{IH} measured at 175–250°C increased slightly with the testing temperature. The texture variation during tube expansion can be explained by the operation of twinning and slip mechanisms. Results of this study have shown that texture modification from the circumferential to the radial one is a very effective alternative method to increase the delayed hydride cracking (DHC) resistance of pressure tube.

1. Introduction

Pressure tubes in a CANDU reactor absorb hydrogen formed by the corrosion process between the pressure tube and the primary coolant, then precipitate hydrides if the hydrogen content is over the terminal solid solubility during operation. It is known that delayed hydride cracking (DHC) is a time-dependent cracking mechanism and that the crack propagates through precipitation and fracture of hydride when there is enough hydrogen and stress. This mechanism has proven to be one of the main causes for potential coolant leakage accidents of pressure vessels in CANDU reactors [1].

There may be several methods to mitigate DHC susceptibility in pressure tubes at the present [2]. These are

1. the reduction of the hydrogen ingress rate by lowering the corrosion rate and by Cr-plating in the rolled-joint between the end fitting and pressure tube,
2. the process of hydrogen ejection using the Pd-plating and the addition of oxygen in the annulus gas system,
3. the modification of texture from circumferential to radial texture.

Although it has been suggested that the radial textured pressure tube would have a higher DHC resistance, and the mitigation of susceptibility on DHC seemed earlier to be one of the useful alternatives [1], there have been few investigations on this topic because of difficulties in the modification of the texture of pressure tubes. It is known that there are no DHC problems in the fuel cladding, because the texture of cladding has already be modified by pilgering processes to a radial texture.

In this paper, the texture of the pressure tube was modified from circumferential to radial texture through the expansion of a CANDU pressure tube using the plain strain fixture; then, the effect of texture modification on K_{IH} was investigated. The effect of texture modification is discussed in terms of deformation mechanisms, and the possible texture modification process is also suggested briefly.

2. Experimental

The pressure tube used in this investigation was expanded 25% using plain strain fixtures designed for tube

* Corresponding author. Tel.: +82-42 868 2061; fax: +82-42 868 8346.

E-mail address: sskim6@nanum.kaeri.re.kr (S.S. Kim).

0022-3115/00/$ - see front matter
PII: S0022-3115(99)00284-6

expansion under the plain strain condition, as shown in Fig. 1. Its thickness was 3.3 mm after the tube expansion. The pressure tube was annealed three times at 580°C for 5 h after 7–8% deformation in order to allow for continued deformation and convenience.

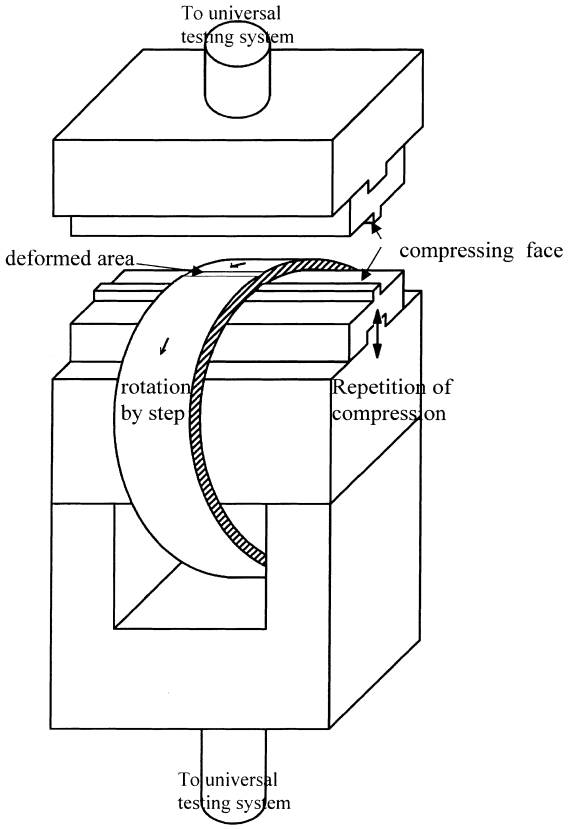

Fig. 1. Schematic diagram of the plain strain fixture for tube expansion.

Tube was compressively deformed by two compressing faces, as shown in Fig. 1. This deformed area shows both compressive and tensile strain in the radial and circumferential direction. Since the upper part of fixture is fixed in universal testing system, the lower fixture can be used to deform the tube. Compressive strain is occurred in the radial direction and most of tensile strain is appeared in the circumferential direction by about 7–8% by one compression when the lower fixture is moved up. The lower fixture is moved down after compression, the compressing faces are opened and then tube is rotated by about the edge width. Again, the lower fixture is moved up, then deformed, and so on.

The texture modification after the tube expansion was confirmed by (0 0 0 2) pole figure measurement using X-ray diffractometer (XRD) under CoK_{α} radiation, and the basal pole components before and after deformation were calculated and compared.

Hydriding was performed in a H_2SO_4 solution electrolytically to form a surface hydride of about 20 μm in thickness, and homogenization was conducted at 300°C for 96 h. Hydrided materials were air-cooled and the hydrogen content was confirmed to be 60 ppm by analysis after homogenization.

The schematic dimensions of the cantilever beam (CB) specimen used to measure K_{IH} is shown in Fig. 2(a), and that of curved compact tension (CCT) specimen is shown in Fig. 2(b) even though this specimens is not tested in this study. The specimens were wire spark-machined after homogenization. Fatigue pre-crack was introduced at the crack tip of the cantilever specimen, and the final K_I at the crack tip was less than 15 $MPa\sqrt{m}$ during pre-cracking. The initial K_I was selected as 17 $MPa\sqrt{m}$ according to testing procedure. The formulae in the calculation of K_{IH} is described in the literature [3].

K_{IH} testing was carried out using the acoustic emission (AE) monitoring method as a crack length to control applied load on the cantilever tester, and applied

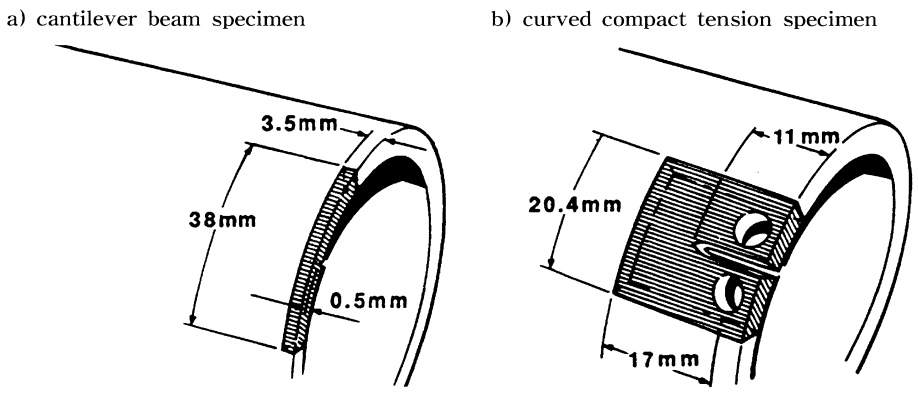

Fig. 2. Schematic illustration of the cantilever beam specimen.

load was reduced by 3% at every 3 μm crack extension. The criterion for K_{IH} was no cracking (AE) for 24 h, and the final K_{IH} was calculated using the final crack length and load after breaking the specimen. The K_{IH} values were measured in the range of 175–250°C, and all specimens were soak-treated at 307°C for 1 h prior to loading.

3. Results and discussion

The optical micrograph is shown in Fig. 3. Grain size became slightly larger during intermediate annealing, and there are some contrasts under polarized light due to grain rotation during the tube expansion process.

The hydride morphology for the radial textured tube is compared with the circumferential in Fig. 4. Even though the magnification between the two different materials is different, it is possible to understand that the hydride platelets of both materials lie mainly in the longitudinal-circumferential plane, except that some hydrides were slightly declined from the circumferential direction in the radial textured tube.

(0 0 0 2) pole figures in the commercial CANDU and the radial textured tube were compared in Fig. 5. (0 0 0 2) poles in the radial textured tube were concentrated 20–30°C from the radial direction, whereas (0 0 0 2) poles in CANDU pressure tube were concentrated in the transverse-radial plane.

The basal pole components in both tubes were compared in Table 1. The basal pole components in the transverse direction, F_T, decreased by 50%, whereas the basal pole components in the radial direction, F_R, increased by about 50% after tube expansion. In addition, the basal pole component in the longitudinal direction was increased about two times.

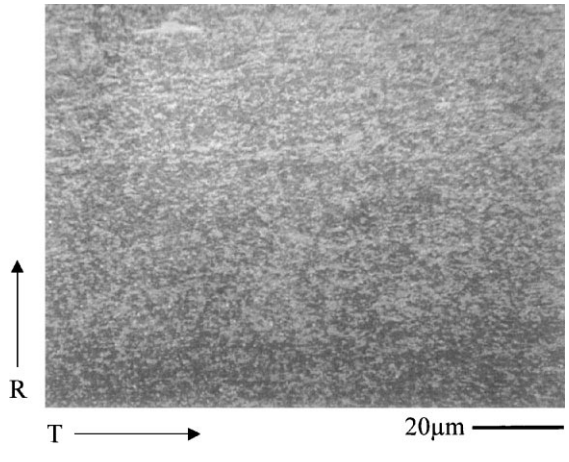

Fig. 3. Optical micrographs of the radial textured tube.

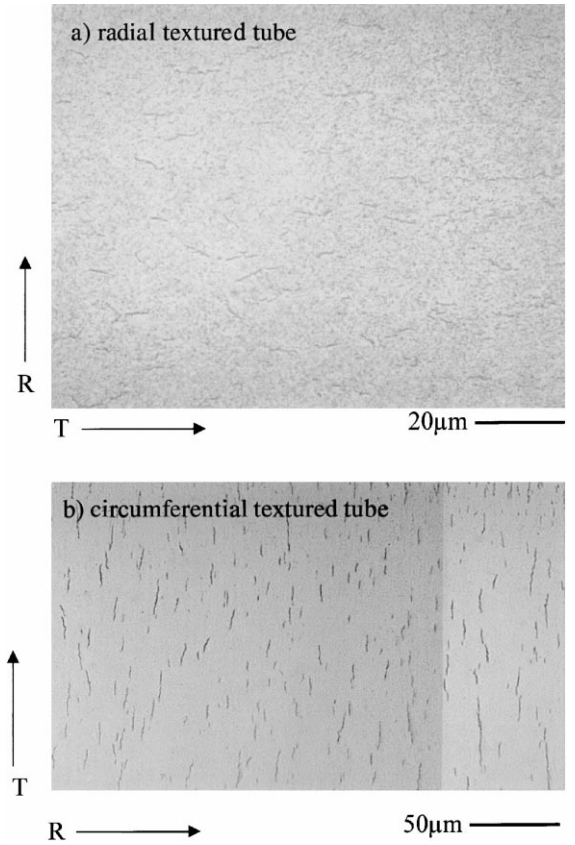

Fig. 4. Hydride morphology of the radial textured and the circumferential textured tube: (a) radial textured tube; (b) circumferential textured tube.

When tube is expanded by plain strain mode, there should be operation of $(10\bar{1}2)$ and $(11\bar{2}1)$ twinning systems. Even though only (0 0 0 2) pole figure is shown in Fig. 5, it is well known that $(10\bar{1}0)$ and $(10\bar{2}0)$ poles are concentrated in the longitudinal and radial direction, respectively. The tensile strain by operation of $(11\bar{2}1)$ system contributes mainly to circumferential direction. However, the tensile strain due to $(10\bar{1}2)$ system contribute to circumferential and longitudinal direction simultaneously, because the (0 0 0 2) poles are rotated by 85° to the radial direction and by 30° to the longitudinal direction at the same time by twinning operation. This is why the basal pole components of the radial textured tube in the radial direction is increased after tube expansion.

The change in texture during tube expansion is achieved by $(10\bar{1}2)$ and $(11\bar{2}1)$ twinning and their slip, since the twinning makes grains prefer slip deformation. The grains parallel to the transverse direction of the tube are preferable to $(10\bar{1}2)$, and the grains whose *c*-axes are declined about 35° are preferable to the $(11\bar{2}1)$ twinning system [4,5], because grains whose *c*-axes are

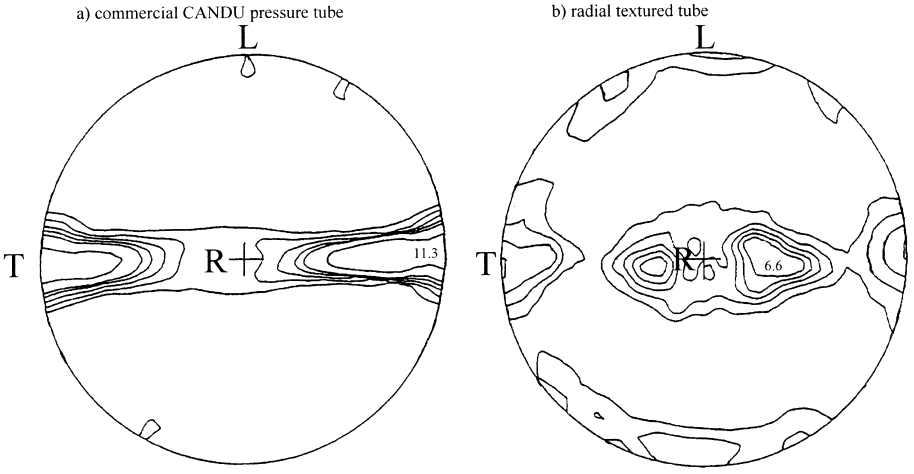

Fig. 5. (0 0 0 2) pole figures of the radial textured tube and the circumferential textured tubes.

Table 1
The basal pole components in the radial and the circumferential textured tubes

Tubes	Basal pole components		
	F_R	F_T	F_L
Circumferential textured tube (commercial CANDU)	0.32	0.59	0.09
Radial textured tube (25% expanded)	0.48	0.32	0.20

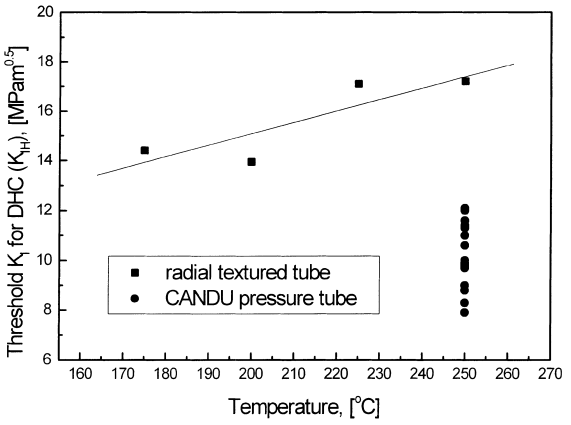

Fig. 6. Temperature dependency of K_{IH} in the radial textured and CANDU tube.

parallel or close to the transverse direction are deformed primarily by twinning rather than by slip. This change was confirmed earlier in Zr–2.5%Nb plate having the similar texture of a pressure tube by cross-rolling [5].

The lowest K_{IH} values in the radial textured tube are plotted in Fig. 6 against the testing temperature. Though it seems that the number of tested temperature were not sufficient, K_{IH} values increase slightly with testing temperature. The K_{IH} at 250°C appeared to be 17 MPa$\sqrt{m}$ to a minimum. This means that the K_{IH} in the radial textured tube is to be at least 70% higher than that of the commercial CANDU pressure tube.

It is known that DHC in Zr-alloys occurs due to the repetition of precipitation of the brittle hydride and its fracture when the hydrogen content is over TSS (terminal solid solubility) at the temperature of the system, and that hydride platelets precipitate in the plane normal to the applied stress and the habit plane of hydride is $(1\,0\,\bar{1}\,7)$ [6]. Thus, DHC behavior is closely related to the texture of Zr-alloys. Furthermore, because (0 0 0 2) poles in the commercial pressure tube are concentrated in the transverse direction, as discussed above, and the interplanar angle between (0 0 0 2) and $(1\,0\,\bar{1}\,7)$ is 14.7°, it is natural that the commercial CANDU pressure tube is susceptible to DHC.

Therefore, the fact that the radial textured pressure tube has a higher K_{IH} can be explained by the lowering of the basal plane density in the cracking plane. This explanation is very consistent with the results observed earlier [5–11]. This can be shown in Fig. 7, in which K_{IH} is plotted against the basal pole component in the stress direction.

It is worth while to note that the K_{IH}s measured from CB specimens in the radial direction are always higher than those of the curved compact tension (CCT) or compact tension (CT) specimens. This seems to be related to the grain orientations at the crack tip during cracking, although the average grain orientations in the cracking plane are the same. The grain orientations at the crack tip in the CB and CT specimens are aligned to the radial and to the longitudinal direction, respectively, as shown in Fig. 5. The grain orientations in the

cracking direction in CCT (or CT) specimen are mostly $(10\bar{1}0)$ and these are very close to each other along the longitudinal direction within 10–15° regardless of the orientation of (0002) pole. However, those in the CB specimen vary from $(11\bar{2}0)$ to $(11\bar{2}4)$ via $(11\bar{2}2)$, and this means that the orientation of neighboring grain may change significantly. This angular range is over 60° in the CB specimen. Since the grain orientations at the crack tip in the CB specimens have much variation compared to the CT specimens, this may inhibit the cracking in the radial direction.

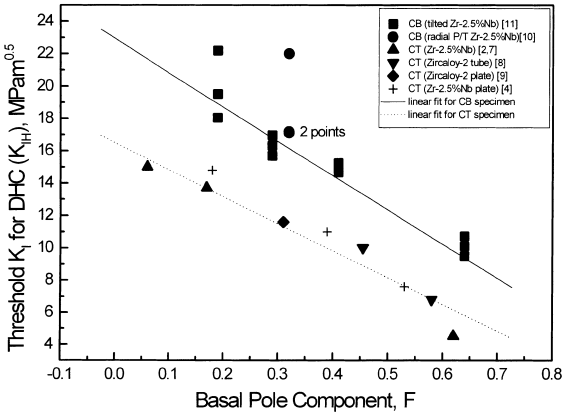

Fig. 7. The basal pole component dependency of K_{IH} in the radial and circumferential textured tube.

The results from the tilted CB specimens were obtained from the tilted CB specimen machined from the flattened pressure tube materials. The tilted CB specimens have different basal pole component from $F = 0.19$ to $F = 0.63$ in the cracking planes. These results show that the minimum K_{IH}s from the various specimen in the radial direction have linear relationship with basal pole components [7].

The low magnified fractographs are compared in Figs. 8–10. They illustrate that the fracture surfaces in the radial textured tube show larger depth variations and a larger portion of ductile fracture compared to the circumferential textured tube. That is, the fracture sur-

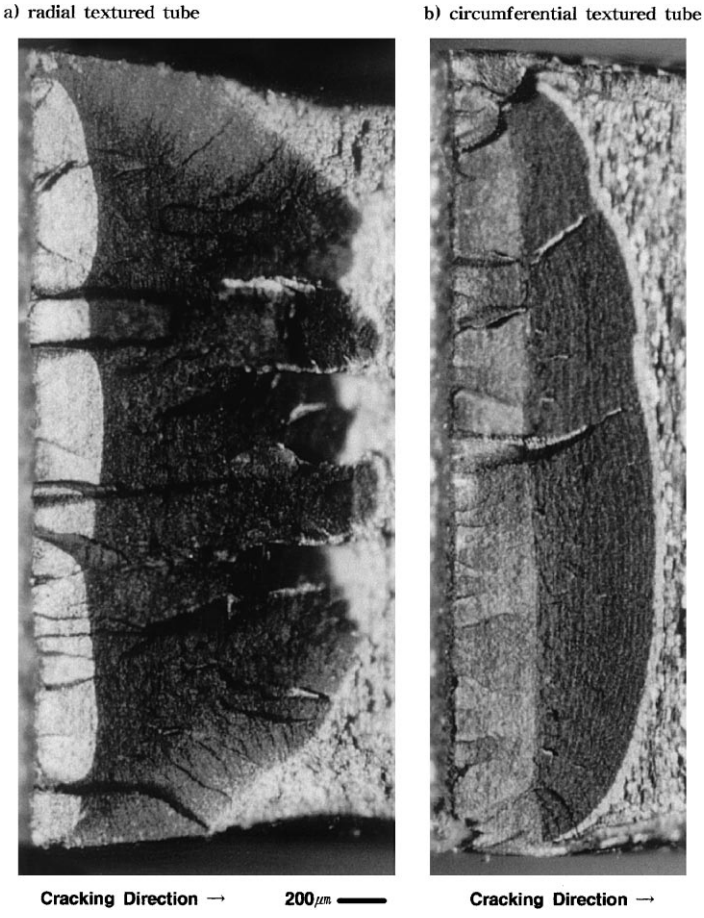

Fig. 8. Comparisons of the optical fractographs of the radial and the circumferential textured tube: (a) radial; (b) circumferential textured tube.

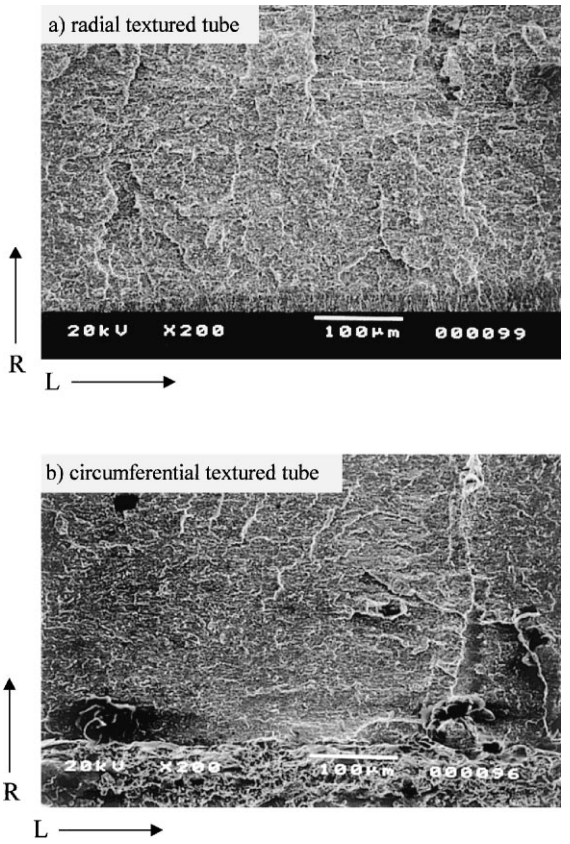

Fig. 9. Comparisons of SEM fractographs of the radial and the circumferential textured tube: (a) radial; (b) circumferential textured tube.

face of the commercial CANDU pressure tube looks flatter and smoother than that of the radial textured tube. The smoothness in the fracture surfaces may represent the ease of crack propagation during the DHC process. This suggests that the denser basal plane in the cracking plane may provide an easier path for the DHC crack. Then, cracking is easier, and thus, the circumferential texture tube would have a lower K_{IH}. But the DHC cracking in the radial textured tube must encounter the lesser basal planes in the cracking plane and propagates through the various grain orientations, compared to the circumferential texture tube. Therefore, the K_{IH} becomes higher when the fracture surface is lesser smooth.

The idea for the texture modification of seamless tube is tube expansion. Although the plain strain fixture was used for small tube expansion in this study, there is a useful method for the large scaled tube like CANDU pressure tube. The manufacturing method of the longer seamless tube with radial texture is available using cross rolling by rotary rolling and/or piercing. This concept is registered as patent in the several countries [12–15].

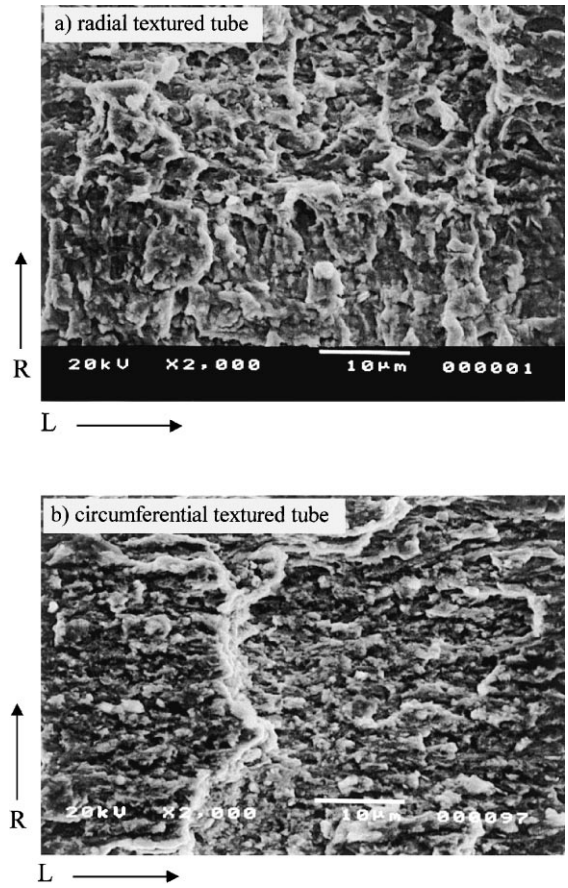

Fig. 10. Comparisons of SEM fractographs of the radial and the circumferential textured tube: (a) radial; (b) circumferential textured tube.

4. Conclusions

It was confirmed that the K_{IH} for DHC initiation in the radial direction in the radial textured pressure tube at 250°C appeared to be 17 MPa$\sqrt{m}$, and this value is at least 70% higher than that of the commercial CANDU pressure tube. This is due to the lesser basal plane close to the habit plane for hydride precipitation in the cracking plane, and this is very consistent with the expectation and the results in the literature. The texture modification of pressure tubes from the circumferential to the radial texture may be a very useful idea to increase the tolerance for DHC initiation and to ensure the safe operation of a CANDU reactor through the increase DHC resistance of pressure tubes in the aspect of DHC.

Acknowledgements

This work has been carried out in the CANDU Pressure Tube Materials project as a part of the Nuclear

R&D program funded by the Ministry of Science and Technology, Korea. The authors would like to acknowledge people working in building #375 in AECL-CRL for their help.

References

[1] C.E. Coleman, J.F.R. Ambler, Zirconium in the Nuclear Industry, ASTM STP 633 (1977) 89.
[2] C.E. Coleman, B.A. Cheadle, C.D. Cann, J.R. Theaker, in: Zirconium in the Nuclear Industry, 11th International Symposium, ASTM STP 1295 (1996) 884.
[3] S. Sagat, J.F.R. Ambler, C.E. Coleman, Atomic Energy Canada Limited Report Number AECL-9258, 1986.
[4] E. Tenckhoff, Deformation Mechanisms, Texture and Anisotropy in Zirconium and Zircaloy, ASTM STP 966, 1988.
[5] S.S. Kim, S.C. Kwon, Y.S. Kim, J. Nucl. Mater. 273 (1999) 52.
[6] V. Perovic, G.C. Weatherly, C.J. Simpson, Acta Metall. 31 (9) (1983) 1381.
[7] S.S. Kim, Y.S. Kim, Y.M. Cheong, S.C. Kwon, K.N. Choo, in: Proceedings of the Korean Nuclear Society Spring Meeting, vol. 225, Pohang, Korea, 1999.
[8] C.E. Coleman, S. Sagat, K.F. Amouzouvi, Control of microstructure to increase the tolerance of zirconium alloys to hydride cracking, Atomic Energy of Canada Limited Report AECL-9524, 1987.
[9] C.E. Coleman, Zirconium in the Nuclear Industry, ASTM STP 754 (1982) 393.
[10] H. Huang, W.J. Mills, Metall. Trans. A 22A (1991) 2149.
[11] W.J. Mills, F.H. Huang, Eng. Frac. Mech. 39 (1991) 241.
[12] S.S. Kim, D.W. Kim, J.W. Hong, Y.W. Kang, Korean patent no. 93725, 1996.
[13] S.S. Kim, D.W. Kim, J.W. Hong, Y.W. Kang, United States patent No. 5681406, 1997.
[14] S.S. Kim, D.W. Kim, J.W. Hong, Y.W. Kang, Canadian patent No. 2126997, 1998.
[15] S.S. Kim, D.W. Kim, J.W. Hong, Y.W. Kang, Japanese patent No. 2921783, 1999.